Environ Geol (2009) 56:935–951
DOI 10.1007/s00254-008-1196-1

ORIGINAL ARTICLE

Hydraulic, textural and geochemical characteristics of the Ajali Formation, Anambra Basin, Nigeria: implication for groundwater quality

Moshood N. Tijani · Matthew E. Nton

Received: 4 October 2007 / Accepted: 8 January 2008 / Published online: 1 February 2008

Abstract This study highlights the distribution of hydraulic conductivity (K) in the regional aquiferous Ajali Formation of SE-Nigeria on one hand and assesses the possible influences of textural and geochemical characteristics on the hydraulic conductivity on the other hand. The investigation approach involved field sampling and collection of 12 sandstone samples from different outcrop locations, followed by laboratory studies such as grain-size analysis (GSA), constant head permeameter test and geochemical analysis of major and trace elements using X-ray fluorescence method. GSA and textural studies show that the sandstones range from fine to medium sands, constituting about <75–99% sand fraction, with graphic mean grain size of 0.23–0.53 mm. Other parameters such as coefficient of uniformity (C_u) range from 1.58 to 5.25 (av. 2.75), while standard deviation (sorting) values of 0.56Ø–1.24Ø imply moderately well sorted materials. In addition, the order of the estimated K values is $K_{permeameter} > K_{Beyer} > K_{Hazen} > K_{Kozeny\text{-}Carmen} > K_{Fair\text{-}Hatch}$ with average values of 1.4×10^{-3}, 4.4×10^{-4}, 3.8×10^{-4}, 2.2×10^{-4} and 8.1×10^{-5} m/s, respectively. These values fall within the range of 10^{-5} and 10^{-3} m/s for fine to medium sands. However, multivariate factor analysis of the data revealed significant positive dependence of the empirically determined K values on graphic mean grain size and percentage sand content and much less dependence on sorting and total porosity. Geochemical profiles of the fresh samples are dominated by quartz with corresponding SiO_2 content of 76.1–98.2% (av. 89.7%) while other major oxides are generally below 1.0 wt.% in the fresh samples. However, the ferruginized samples exhibited elevated concentrations of Al_2O_3 (3.50–11.60 wt.%) and Fe_2O_3 (1.80–3.60 wt.%), which are clear indications of weathering/ferruginization processes with attendant trace metal release/enrichment (2.5 mg/l Cu, 7.5 mg/l Pb, 6.5 mg/l Zn, 3.9 mg/l Ni and 19.6 mg/l Cr) call for concern in respect of the chemical quality of the groundwater system. The associated groundwater is generally soft, slightly acidic, and with low dissolved solids (EC = 14–134 µs/cm) dominated by silica; implying water from clean sandy aquifer devoid of labile and weatherable minerals. Nonetheless, most of the metals (with exception of Si, Fe and Mn) exhibited higher degree of mobility (2–12 folds), which can be attributed to reduction of Fe-/Mn-oxyhydroxides as sinks/hosts for trace metals. Consequently, infiltration-induced geochemical reactions (redox, ferruginization and leaching processes) signify potential environmental impact in terms of groundwater quality as well as borehole/aquifer management, especially under humid tropical environment of the study area.

Keywords Hydraulic conductivity · Permeability test · Geochemical profile · Metal enrichment · Groundwater chemistry · Ajali Formation · Anambra Basin · Nigeria

Introduction

Sandy aquifers, either consolidated or unconsolidated are known to be prolific sources of groundwater all over the world. However, long-term sustainable management of the groundwater resources, in terms of quantity and quality, in such aquifer settings requires reliable knowledge of textural characteristics and hydraulic conductivity (K) with respect to groundwater flow and storage. This is in addition

M. N. Tijani (✉) · M. E. Nton
Department of Geology, University of Ibadan, Ibadan, Nigeria
e-mail: tmoshood@yahoo.com; mn.tijani@mail.ui.edu.ng

to possible geochemical interactions between the aquifer matrix and groundwater which may be a critical factor controlling the chemical composition and quality of the water. Furthermore, to adequately understand the groundwater flow condition as well as the movement of dissolved contaminants in the subsurface (aquifer), also requires reliable information on the magnitude of the hydraulic conductivity (K) of the aquifer system.

Several laboratory and field methods are in use for characterization of hydraulic properties of aquiferous sedimentary units. There have been advances in the field-scale methods of measurements and evaluation of hydraulic properties in different aquifer settings/conditions (Bouwer and Rice 1976; Butler 1997; Butler and Garnett 2000; Angeroth 2002) on one hand. On the other hand, simple laboratory procedures and empirical estimations are still considered useful and cheaper means of estimating hydraulic conductivity (K) in hydrogeological studies. Although in-situ determination of K could be more accurate and reliable in site-specific investigations, laboratory approaches are usually preferred in many instances, especially during preliminary hydrogeological investigations, in order to cut down on cost and time. Nonetheless, lack of funds for field scale operation, as well as inadequate experimental laboratory facilities are serious limitations in developing countries like Nigeria. In this regard, simple procedures and empirical estimation of parameters could be seen as appropriate alternative to generate some basic hydrogeological data. However, there is the need to assess the limitations and level of accuracy of empirical estimations in respect of actual field situations.

Furthermore, geology controls much of the natural distribution of chemical constituents in groundwater system; hence the natural quality of groundwater will depend on rock/aquifer types and there is a scope of geochemical interactions between the water and the aquifer matrix along the flow paths (Hudson and Golding 1997; Toth 1999; MacDonald et al. 2005; Glynn and Plummer 2005; Appelo and Postma 2005). Such chemical interactions are usually mediated by infiltrating/recharge rainwater that dissolves carbon dioxide to produce weak carbonic acid that can remove soluble minerals from the aquifer matrix (Llyod and Heathcote 1985). Therefore, it may be possible to infer the likelihood of occurrence of certain chemical constituents, not only on the basis of the underlying/associated geologic unit, but also on the basis of possible geochemical reactions/conditions. For example, studies had shown that geo-pedological weathering/ferruginization reactions can lead to metals' release into the environment, while reducing conditions as obtained in the groundwater zone can promote the mobilization of metals that are of environmental and health significance into the groundwater (Bruand 2002; Smedley and Kinniburgh 2002; Tijani et al. 2006). This study therefore highlights the geochemical characterization of both fresh and ferruginized units of the Ajali Formation and possible implications of the associated metal enrichment and mobility vis-à-vis groundwater quality.

In summary, this study therefore highlights the distribution of hydraulic conductivity (K) in the regional aquiferous Ajali Formation SE-Nigeria through comparative assessment of estimated hydraulic conductivity (K) from grain size analysis (GSA) and laboratory permeability tests on one hand. On the other hand, utilizing an integrated textural and geochemical approach, possible ferruginization-induced metal enrichment, potential mobilization with respect to the groundwater composition/quality as well as hydraulic characterization of the Ajali Formation are also highlighted. Consequently, the scope and purpose of this study are:

(a) to present the magnitudes and distribution of hydraulic conductivity values estimated from both laboratory permeameter tests and GSA-based empirical estimations,
(b) to highlight the geochemical composition as well as weathering characteristics of the Ajali Formation,
(c) to highlight possible influence of the recharge-induced ferruginization and geochemical processes on the Ajali Formation and
(d) to assess possible influence of ferruginization-induced metal mobility on groundwater quality as well as borehole/aquifer management.

Study area

Geologic and stratigraphic settings

The Ajali Formation is one of the lithostratigraphic units in the Anambra Basin, SE Nigeria. The Anambra Basin is a Cretaceous sedimentary basin, located in the southeast portion of Nigeria and bounded by the Abakaliki anticlinorium of the southern Benue Trough to the east and by the Basement Complex of the southwestern Nigeria to the west (Fig. 1). Geologically, the origin of the Anambra Basin is intimately related to the tectonic and sedimentary cycles responsible for the origin of the adjoining southern Benue Trough during the separation of African from the South American plate in the Mesozoic era (King 1950; Reyment 1965; Burke et al. 1972; Benkhelil 1986). The general geological map of the Upper Cretaceous sedimentary succession within the Anambra Basin is presented in Fig. 1.

Studies of Murat (1972), Nwachukwu (1972) Hoque and Ezepue (1977) and Ladipo (1986, 1988) among others, have shown that, subsequent to the uplift of the Benue-

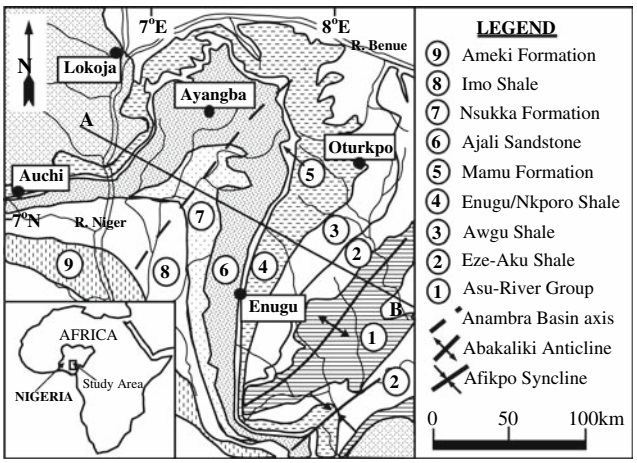

Fig. 1 Geological map of Anambra Basin showing the different sedimentary units. (A–B line of cross-section in Fig. 3)

Abakaliki fold belt during the Santonian, the geological history of the Anambra Basin is linked to the post-Santonian subsidence of the then Anambra platform. This was followed by a series of trans-regression cycles leading to sedimentation of about 6 km thick of Cretaceous and Tertiary sediments (Obaje et al. 1999) within the basin to the west of the Abakaliki uplift during the Campanian—Paleocene. A summary of the stratigraphic relationship of the main sedimentary units within the basin is presented in Fig. 2 and brief descriptions presented below:

(a) *Enugu-Nkporo Shales Group*: These early Campanian units underlie the eastern plain of the Udi-Enugu escarpment and consists of dark grey fissile, soft shale and mudstone with maximum thickness of about 1,000 m and characterized by interbedded sandy units and sulfur coated marl. A shallow marine environment was predicted due to the presence of foraminifera and ammonites (Reyment 1965; Agagu et al. 1985).

(b) *Mamu Formation*: This is a Late Campanian sedimentary unit, also known as the "Lower Coal Measures". It consists of mainly dark blue to grey shales/mudstones units with alternating sandy units and coal seam horizons to form a characteristically stripped rock unit. The Mamu Formation was deposited as shallow water of the paralic facies of a deltaic complex (Cratchley and Jones 1965).

(c) *Ajali Formation*: This is a Maastrichtian sandy unit overlying the Mamu Formation and consists of white, thick friable, poorly sorted cross-bedded sands with thin beds of white mudstone near the base. It is characterized by large scale cross bedding with dip angle as high as 20°. Studies have suggested that the Ajali Formation is a continental/fluvio-deltaic sequence, characterized by a regressive phase of a short-lived Maastrichtian trans-regression with sediments derived from westerly areas of the Abakaliki anticlinorium and the granitic basement units of Adamawa-Oban massifs to the eastern side of the basin (Benkhelil 1986; Amajor 1987; Ladipo 1986, 1988; Adediran 1991). Further details in respect of the Ajali Formation, as the focus of this study, is presented below under the section on hydrogeologic setting.

(d) *Nsukka Formation*: This is a Late Maastrichtian unit, lying conformably on the Ajali Formation and consists of alternating succession of sandstone, dark shales and sandy shales with thin coal seams at various horizons, hence termed the "Upper Coal Measures". The sedimentary successions indicate a paralic environment.

Physiography and drainage

Within the Anambra Basin, the topography is generally lowly undulating, with elevations of about 150–250 m above sea level. As shown in the cross-sectional view of the Ajali Formation alongside other lithostratigraphic units (Fig. 3), the most prominent relief feature in the study area is the N–S trending Udi-Enugu escarpment at the eastern edge of the basin, which rises to an average elevation of about 400 m above sea level. This slopes to the west at less than 30° towards the main area of the basin with lowly undulating topography characterized by elevation of about

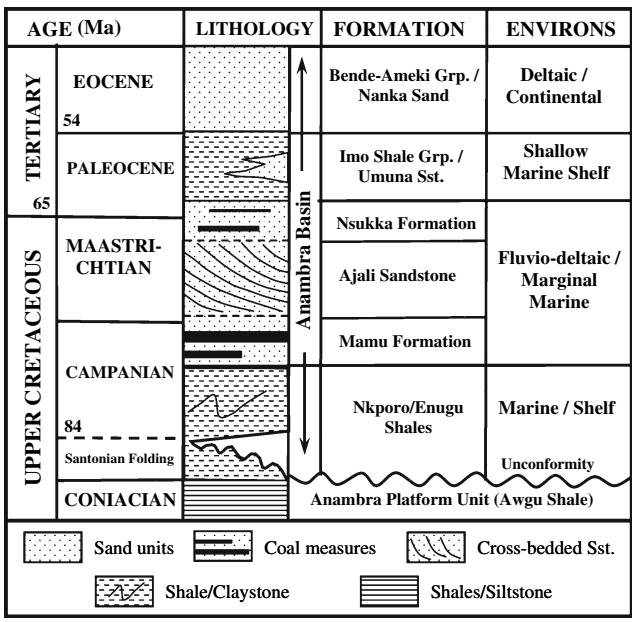

Fig. 2 Stratigraphic profiles and depositional environment of the sedimentary units within the Anambra Basin

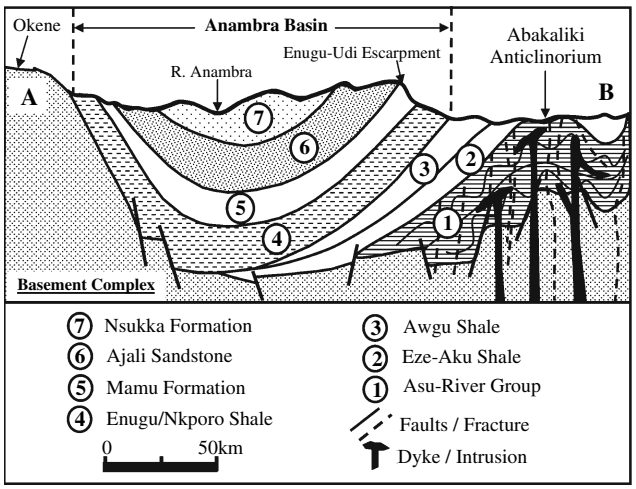

Fig. 3 A cross-sectional view of the sedimentary units within the Anambra Basin (line of section A–B in Fig. 1)

150–250 m above sea level while the scarp slope towards the east dips at high angles of about 60–70° (Uma and Onuoha 1988; Okogbue 1988). Generally, this relief feature is dissected by numerous gullies resulting in a characteristic rugged terrain.

In terms of the drainage setting, the crestal zone of Udi-Enugu escarpment serves as water divide; the western side is characterized by hummocky terrain of the Adada-Aghawinili River Basin with headwaters such as Adada, Mwuyi, Ajali, Mamu, Karawa and Oji Rivers as tributaries of the River Niger. The slopy eastern side of the escarpment is drained and dissected by the gullying drainage system such as Iyakwa, Atafo, Iyoko, Awra, Eme and Iddo Rivers.

Hydrogeologic settings

The general geology and physiography of the Anambra Basin controls the occurrence of groundwater in the study area. This falls into two hydrogeologic groups:

(a) *First hydrogeologic group*: Areas underlain by the predominantly shaly formations (i.e., Enugu-Nkporo Shale, Mamu Formation) to the east of the Udi-Enugu escarpment.
(b) *Second hydrogeologic group*: Areas underlain by predominantly sandy horizons (Ajali and Nsukka Formations) to the west and northwest of the Udi-Enugu escarpment.

The first hydrogeologic group is characterized by unconfined shallow aquifer of the upper weathered horizon in continuity with the fractured shales and intercalated sandy horizons. Uma and Onuoha (1988), noted that aquifers in this group support only dug wells (with saturated thickness of about 1.3 to about 3.8 m) and shallow hand-pump boreholes (usually less than 50 m deep) with average capacity of about 2.0 m^3/h. However, deep boreholes with motorized pumps are characterized by intermittent yield ($Q < 5.0$ m^3/h), indicating limited capacity of the unconfined shallow aquifer east of Udi-Enugu escarpment. However, the second hydrogeologic group is characterized by the occurrence of a deep and thick confined and semi-confined Ajali Formation aquifer, which is the main focus of this study.

Hydrogeologically, the cross-bedded Ajali Formation is an extensive regional aquiferous stratigraphic unit (Reyment 1965) and composed of Maastrichtian sand unit, that serves as an important source of water resource within the Cretaceous Anambra Basin. It conformably overlies the Mamu Formation, and is partly overlain by the Late Maastrichtian Nsukka Formation, that is characterized by alternating sandy and shaly units. The Ajali Formation outcrops and extends from Fugar/Agenebode area in the west and extends eastward along the Enugu-Udi escarpment where groundwater is recharged (Okagbue 1988) and narrows southwards towards Okigwe area forming a characteristic "question mark" shape (see Fig. 1). The thickness ranges from over 350–450 m in places and thins southward to few tens of meters around Okigwe area (Hoque and Ezepue 1977). Field study has shown that the upper portion of the Ajali Formation is ferruginized in places; this alongside with the clay/shale unit of the overlying Nsukka Formation and the basal Mamu Formation favours the development of confined/semi-confined aquifer.

The major hydrogeologic feature is the occurrence of a deep and thick confined and semi-confined aquifer, especially in areas directly overlain by the Nsukka Formation, while unconfined conditions exist only in the outcrop areas of the Ajali Formation. In addition, occurrence of localized perched aquifer systems are said to be common in areas where the lateritized Nsukka Formation occurs as outliers on the Ajali Formation (Uma and Onuoha 1988). Most of the boreholes tapping this deep aquifer have depths of about 120–200 m and saturated thickness in the range of 42–150 m, while the yields vary from 10 to 100 m^3/h (Okagbue 1988). In addition, transimssivity values of 1.0×10^{-2} to 1.7×10^{-2} m^2/s and storativity of about 0.02 (Egboka and Uma 1986) are indications of the prolific nature of the Ajali Formation aquifers. The potentials of the aquifer, however, appear to decrease westwards due to decrease in thickness as also noted through hydrogeophysical investigations (Uma and Onuoha 1988; Okagbue 1988). Nonetheless, it should be pointed out that the friable and permeable characters of the Ajali Formation is consequential to environmental land degradation in form of gully erosions in some areas as highlighted by Nwajide (1979); Nwajide and Hoque (1979) and Uma and Onuoha

(1988). This also implies problems in terms of shallow groundwater occurrence in some area, due to its relatively high permeability that allows complete drainage of water to the deeper section of the formation.

Methodology

Field sampling, laboratory tests and analyses

A hydrogeological reconnaissance field survey of the Anambra Basin was undertaken. The field study trip covered most of the outcrop areas of the Ajali Formation and entailed collection of representative samples from 12 different locations as shown in Fig. 4. It should be noted that due to the friable nature of the Ajali Formation, it was difficult to collect undisturbed samples. Hence, samples were collected from outcrop sections (using grab/scooping auger) in deep sand quarry pits and road cuts. Details of lithologic logs of some of the sample locations are presented in Fig. 5. Furthermore, the selection of the 12 representative samples across the outcrop stretches of the Ajali Formation (see Fig. 4) was considered adequate in view of the seemly homogenous and similar characteristics of the Ajali Formation.

In addition, ten representative groundwater samples from different water wells (boreholes) tapping the aquifer (see Fig. 4) were also collected in sterilized plastic bottles, appropriately acidified and preserved prior to chemical analyses of dissolved metal concentrations. Although, details lithologic logs of the sampled boreholes were not available, the field information shows that the wells in sample locations 1, 3, 4, 5, 6. 9 and 10 are deep boreholes (100–120 m), apparently tapping the fresh aquifer unit while locations 2, 7 and 8 are characterized by shallower boreholes (20–30 m) tapping the ferruginized upper section of the Ajali Formation, Subsequent to the field sampling operations, laboratory grain size analysis (GSA), permeameter tests, geochemical analyses of major and trace elements of both fresh and ferruginized outcrop samples of the Ajali Formation as well as the hydrochemical analyses of the groundwater samples were carried out.

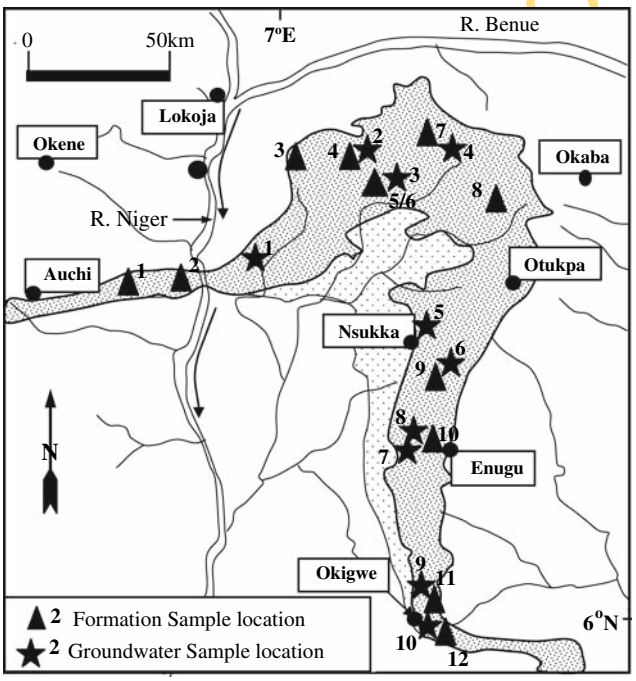

Fig. 4 Map of the Ajali Sandstone Formation (ASF) showing both the rock unit sand groundwater sample locations

For the GSA, the collected samples were air-dried and since the samples were friable, disaggregation was done with fingers. This was followed by sieve analyses using standard laboratory procedure (ASTM D-422). Cummulative curves were plotted from the GSA data and relevant statistical and textural parameters were also deduced. In addition, laboratory determinations of hydraulic conductivity were carried out using the constant head permeameter tests following standard procedure (ASTM D-2434). The set-up of the permeameter tests was based on the principle of Darcy's experiment, which established the relationship between the flux of water through a porous medium and the hydraulic head difference at both ends of the medium. For the porosity determination, the weight of dry sample of the Ajali Formation filled into the permeability tube (cylinder) of known weight was recorded before addition of water for saturation. The saturated sample and the cylinder were weighed, while the volume of the saturated sample was recorded. The difference between the volume of saturated sample and dry sample noted gives the pore volume and the porosity was calculated accordingly.

Following appropriate sample preparation/filtration, the acidified groundwater samples from the Ajali aquifer were subjected to hydrochemical analyses of the major and trace metals concentrations using ICP-OES technique. For the analyses of major and trace elements composition, samples were subjected to appropriate treatment by homogenization of 2 g of each sample with 4 g of analytical *spectroflux* powder and 0.6 g $LiNO_3$ salt in agate mortar. The mixture was then subjected to heat fusion and glass beads preparation in platinum plate (3.5 cm diameter) using bead and fuse sampling machine (model TK-410, Rigaku-Tokyo). The respective glass beads were then used for the determination of major and trace elements using automated X-ray fluorescence (XRF) machine (model *Rigaku ZSX*).

The GSA, permeability and porosity tests were performed at the Department of Geology, University of Ibadan, Nigeria. The geochemical XRF analyses were carried out at the Department of Earth and Planetary

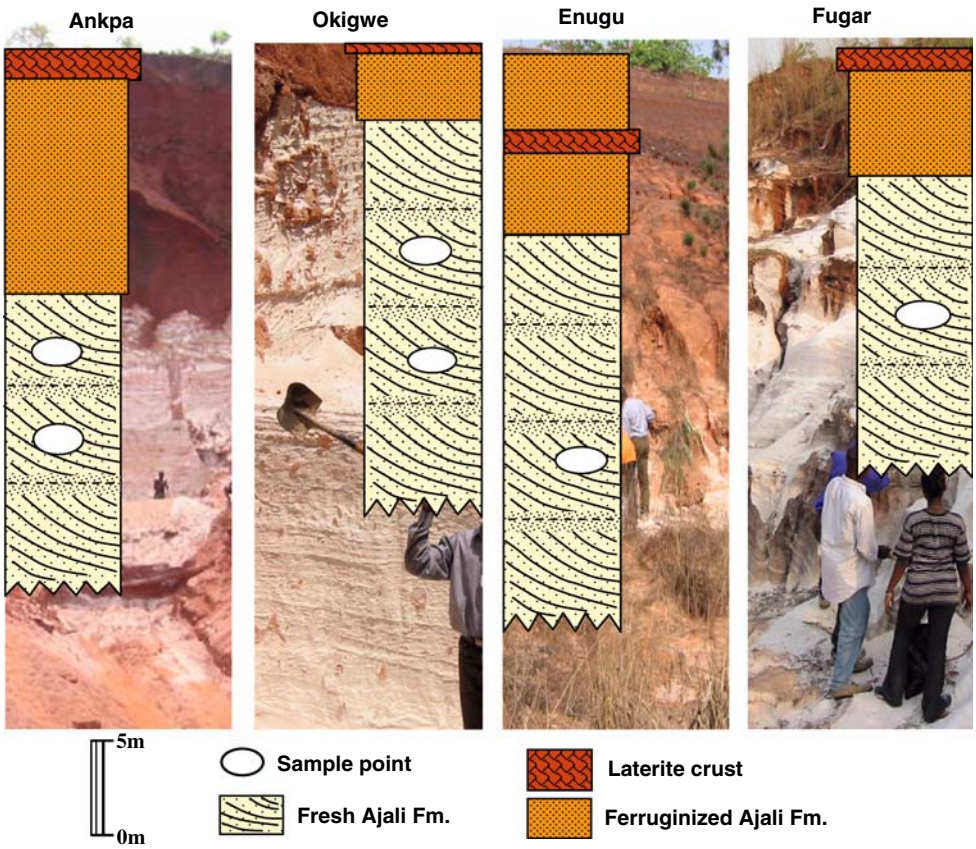

Fig. 5 Representative lithologic profiles of some of the sample locations

Science Systems, Hiroshima University, Japan, while the hydrochemical analyses of the associated groundwater samples were carried out at the Activation Laboratory, Ontario in Canada.

Data evaluation

In line with the above laboratory studies, data evaluation and estimations of some indices were subsequently undertaken. Using the laboratory data from the permeameter tests, the respective hydraulic conductivity values (K) were calculated using the following Darcy (1856) relation:

$$K = Q/A * \mathrm{dl}/\mathrm{dh}$$

where

A cross-sectional area of sample (m^2)
dl L = length of sample chamber (m)
Q volumetric flow rate = volume of water released/time (m^3/s)
dh ($h_f - h_0$) = difference between initial head and final head (m).

From the GSA results and the respective cumulative curves, estimation of some textural indices (uniformity coefficient and coefficient of curvature) and statistical parameters such as sorting, skewness, kurtosis, etc. were undertaken using following the relations of Folks and Ward (1957):

Graphic mean: $M = (\varnothing_{16} + \varnothing_{50} + \varnothing_{84})/3$

Inclusive graphic skewness:

$$S = \frac{(\varnothing_{84} + \varnothing_{16} - 2(\varnothing_{50})}{2(\varnothing_{84} - \varnothing_{16})} + \frac{(\varnothing_{95} + \varnothing_{5} - 2(\varnothing_{50})}{2(\varnothing_{95} - \varnothing_{5})}$$

Inclusive graphic standard deviation:

$$D = [(\varnothing_{84} - \varnothing_{16})/4] + [(\varnothing_{95} - \varnothing_{5})/6.6]$$

Graphic kurtosis: $M = \dfrac{(\varnothing_{95} - \varnothing_{5})}{2.44(\varnothing_{75} - \varnothing_{25})}$

Uniformity coefficient: $C_u = D_{60}/D_{10}$

Coefficient of curvature: $C_c = (D_{30})^2/(D_{10} \times D_{60})$

Notation: The subscript in the phi terms (ϕ_x) refers to the grain size at which x% of the sample is coarser than the specified size, or also, the size at which x% of the sample is retained on a specified sieve size and any coarser screened sieves above that particular sieve. Also Dx terms represent the respective grain diameter in mm, for which x% of the sample is finer than.

Due to the importance of K in the fields of hydrogeology, petroleum geology, and water and waste-water engineering, a number of studies had empirically related K

to the particle size distribution of unconsolidated materials (e.g., Hazen 1892, 1930; Krumbein and Monk 1942; Fair and Hatch 1933; Beyer 1964; Shepard 1989; Alyamani and Sen 1993) among others. Detailed review of some of these methods, their applications and limitations can be found in Egboka and Uma (1986); Uma et al. (1989) and Lee (1998). A common aspect of those studies is the determination of an empirical relationship between the hydraulic conductivity and some statistical textural parameters such as the geometric mean, mode, standard deviation (dispersion), or effective diameter etc. of the aquifer materials. The applicability of these empirical formulae in this study is based on the fact that these empirical relations are based on granular sandy materials as also exemplified by Ajali Formation aquifer. Consequently, as part of data evaluation, four of such existing empirical relations were employed as presented below:

Hazen (1930): $K_{\text{Hazen}} = C(D_{10})^2$
Beyer (1964): $K_{\text{Beyer}} = [g/\upsilon]C_b \times D_{10}{}^2$
Kozeny-Carmen (in Carmen 1939): $K_{\text{K-Carmen}} = (\rho g/\upsilon)[n^3/(1-n)^2]\ (D_m{}^2/180)$
Fair and Hatch (1939): $K_{\text{F-Hatch}} = (\rho g\ /\upsilon)\ [n^3/(1-n)^2] \times 1/m(\theta/100 \times \Sigma\ P_i/D_i)$

Notations

K hydraulic conductivity (in cm/s or m/s or m/day).
C a dimensionless coefficient based on grain size and sorting character.
D_{10} grain size for which 10% of grains are finer (effective grain size);
D_{50} grain size for which 50% of grains are finer;
C_b a coefficient defined as $6.0 \times 10^{-4} \times \log_{10}(500/C_u)$;
υ viscousity of the fluid water (0.01 g/cm s);
g acceleration (980 cm/s^2);
C_u uniformity coefficient;
ρ density of the fluid;
D_m representative grain size;
n porosity;
m packing factor, experimentally determined as 5;
θ shape factor (6 for spherical grains and as 7.7 for angular grains);
Pi % by weight of grains held between sieves;
Di geometric mean size of grains held between the sieves.

Results, interpretations and discussions

Textural and statistical indices

The plots of cumulative curves of representative samples of the grain size distribution of the Ajali Formation from different outcrops within the Anambra Basin are presented in Fig. 6, while the results of the estimated textural and statistical indices are presented in Table 1. As shown in Table 1 and also presented in Fig. 6, the sandstone under study falls predominantly within uniform medium sand range. This is clearly supported by the graphic mean (G_m) of 0.98–1.98 φ; with the exception of sample from Dekina, having graphic mean of 2.26 φ, which implies fine sand and apparently attributable to weathering influence. However, the estimated inclusive graphic standard deviation (D) ranges from 0.55 to 1.29 φ, suggesting a wider range from poorly sorted to moderately well-sorted material. Also varied values of inclusive graphic skewness from −0.24 to +0.20 (av. 0.02) imply nearly symmetrical to coarse skewed arrangement while graphic kurtosis (KG) ranges from 0.94 to 1.51 φ (av. 1.20) and suggest mesokurtic through leptokurtic with majority of the samples having leptokurtic population.

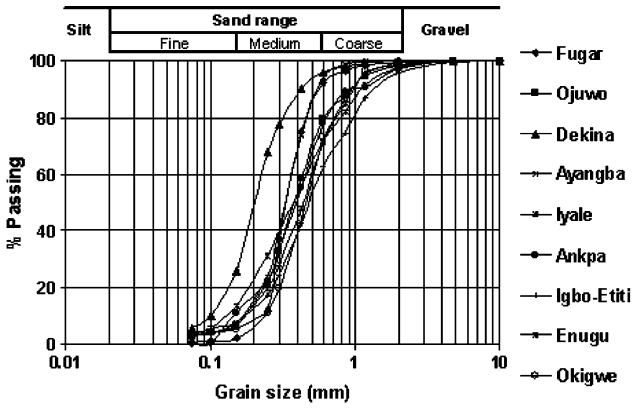

Fig. 6 Representative grain size distribution curves of the ASF

For the textural indices, the uniformity coefficient (C_u), which provides a measure of uniformity of the grain sizes ranges from 1.58 to 5.25 while the coefficient of curvature (C_c) ranges between 0.89 and 1.57. However, the samples from Okigwe-Uturu-1 have relatively higher values of 5.25 and 1.57 for Cu and Cc respectively (see Table 1). This alongside with 25% fines imply relatively poorer hydraulic characteristic at the Okigwe-Uturu-1 area compared to other sample locations. Budhu (2000) pointed out that C_u value <4 implies uniform grading of grains with enhanced drainage/permeability, and values >4, indicate a wider assortment of grain sizes. In this study, C_c values between 1 and 3, coupled with uniformity coefficient greater than zero ($C_u > 0$), indicates a well-graded granular material. Furthermore, the % fines of 0.3–6.0, porosity of 25.5–32.8%; % sand of >94% are clearly consistent with the range of values for medium sands (Table 1). Nonetheless, the % fine of 24.9% and a lower porosity of 18.0% for the Okigwe-Uturu-1 sample (Table 1) is a pointer to the relatively higher values of C_u and C_c compared to other samples. By and

Table 1 Results and summary of statistical and textural indices based on GSA data (sample code same as given in Table 2)

Location	Gmean (φ)	IGStd. (φ)	IGSkw.	Gkurt.	Cu	Cc	n (%)	% Fine	% Sand
Fugar-Agenebo-I	1.48	0.55	0.20	1.51	1.58	0.92	27.9	0.6	99.4
Fugar-Agenebo-II	1.96	0.61	0.18	0.94	1.75	0.89	nd	1.6	98.4
Ojuwo	1.41	0.94	0.01	1.22	2.53	1.15	25.5	3.0	97.0
Ayangba-Ia	1.63	0.70	−0.24	1.38	2.24	1.21	32.8	3.1	96.9
Ayangba-Ib	1.43	0.74	0.12	1.02	2.21	1.05	nd	1.4	98.6
Iyale	1.36	1.28	0.04	0.99	3.43	0.93	nd	3.8	96.2
Ankpa	1.45	1.07	−0.01	1.38	3.07	1.22	27.9	0.3	99.7
Igbo-Etiti-I	0.98	1.29	−0.05	1.23	3.28	1.09	nd	4.3	95.7
Enugu-Km8-Ia	1.21	1.01	−0.10	0.96	3.00	1.11	29.4	2.8	97.2
Okigwe-Uturu-I	1.69	0.64	nd	nd	5.25	1.57	18.0	24.9	75.1
Okigwe-Uturu-IIa	1.10	0.87	−0.04	1.34	2.08	0.94	32.6	3.4	96.6
Dekina-I	2.26	0.82	0.07	1.40	2.30	1.26	nd	6.0	94.0
Minimum	0.98	0.55	−0.24	0.94	1.58	0.89	18.0	0.3	75.1
Maximum	2.26	1.29	0.20	1.51	5.25	1.57	32.8	24.9	99.7
Mean	1.50	0.88	0.02	1.20	2.73	1.11	27.4	4.6	95.4

Gmean graphic mean (φ)
IGStd. inclusive standard deviation (φ), *IGSkew.* inclusive graphic skewness, *Gkurt.* graphic kurtosis, *Cu* uniformity coefficient, *Cc* coefficient of curvature, *n* porosity (%)

large, from the textural and statistical indices, the Ajali Formation can be interpreted as uniformly and moderately graded medium sand materials, with high hydraulic potentials in terms of groundwater recharge.

Empirical *K*-values estimations and permeameter tests

Results of hydraulic conductivity (m/s) estimations using different empirical (GSA-based) relations and that from the laboratory permeameter tests are presented in Table 2. The estimated GSA-based *K*-values revealed a minimum range of 2.9×10^{-5}–1.1×10^{-4} m/s (Fair-Hatch method) and a maximum range of 7.4×10^{-5}–8.8×10^{-4} m/s (Beyer method). These are in slight contrast to the range of 3.11×10^{-4}–3.0×10^{-3} m/s, obtained from the laboratory constant head permeameter tests (Table 2). The relatively higher values for the permeameter tests may be attributed to the possible effects of sample repacking and loss/removal of fines with drainage water during the tests. However, among the empirical estimations, only Fair-Hatch approach yielded values comparable to the field pumping/aquifer test data compiled from Okagbue (1988) and presented in Fig. 7 alongside other *K*-estimations. This can be attributed to the fact that the Fair-Hatch relation takes into account the different grain size fractions and the shape factor, which seems to be a better approximation of the in-situ packing conditions under the influence of the overburden pressure. Generally, the observed trend of different estimations is $K_{\text{permeameter}} > K_{\text{Beyer}} > K_{\text{Hazen}} > K_{\text{Kozeny-Carmen}} > K_{\text{Fair-Hatch}}$, with corresponding average values of 1.4×10^{-3}; 4.1×10^{-4}; 3.6×10^{-4}; 2.1×10^{-4} and 7.6×10^{-5} m/s, respectively (see Table 2). Nonetheless, it can be seen that the values from the laboratory permeameter tests and those from the empirical estimations for the Ajali Formation fall within a range of 10^{-4}–10^{-6} m/s (10^{-1} to 10^{-3} m/day) for clean sands; interpreted to be permeable to highly permeable (Freeze and Cherry 1979). Furthermore, the estimated *K*-values from both laboratory permeameter tests and empirical estimations are comparable to similar aquiferous materials such as Nanka Sands with $\sim 8.1 \times 10^{-5}$–1.4×10^{-4} m/s ($\sim$7–75 m/day), Benin Formation with $\sim 6.9 \times 10^{-5}$–9.3×10^{-4} m/s ($\sim$6–80 m/day) and Lokoja Sandstone with $\sim 3.5 \times 10^{-5}$–8.1×10^{-4} m/s ($\sim$3–70 m/day) (Okagbue 1988; Vrbka et al. 1999) as also graphically presented in Fig. 7. It can be concluded, however, that properly conducted laboratory determination and empirical estimations of *K*-values can be taken as cheaper means of generating reliable hydraulic parameter data in absence of field or in-situ measuring facilities as obtained in most developing countries like Nigeria.

Statistical reduction of textural parameters and hydraulic conductivity

In this study, multivariate factor analysis was employed for assessment of interrelationship between the textural-statistical indices and the hydraulic conductivity. The application of multivariate statistical methods for classification and interpretation of large hydrological data set, allows for the reduction of the dimensionality of the data and extraction of few component factors for simplification

Table 2 Results of hydraulic conductivity (m/day) estimations using different empirical relations and permeameter tests

Code No.	Location	*K*-lab	*K*-Beyer	*K*-Hazen	*K*-KC	κ-FH	*k*-Darcy
AJSt-01	Fugar-Agenebo-I	142.5	73.1	59.7	16.0	8.0	45.6
AJSt-02	Fugar-Agenebo-II	62.8	31.9	26.5	6.9	4.3	17.9
AJSt-03	Ojuwo	258.8	33.7	30.0	18.0	7.3	30.8
AJSt-05a	Ayangba-Ia	81.5	34.5	30.0	12.6	5.8	29.2
AJSt-06a	Ayangba-Ib	147.8	43.2	37.4	17.5	8.1	38.5
AJSt-07	Iyale	55.3	21.5	20.3	19.6	5.8	21.4
AJSt-08	Ankpa	143.1	25.3	23.3	16.9	7.7	24.3
AJSt-09a	Igbo-Etiti-I	182.8	35.9	33.6	36.4	9.0	39.1
AJSt-10a	Enugu-Km8-Ia	99.1	32.6	30.0	25.2	8.2	39.4
AJSt-12	Okigwe-Uturu-I	67.3	6.4	6.6	11.3	2.6	28.6
AJSt-13a	Okigwe-Uturu-IIa	157.5	75.6	64.8	29.9	9.7	55.5
AJSt-04a	Dekina-I	26.9	11.9	10.4	3.7	2.5	7.2
Minimum		26.9	6.4	6.6	3.7	2.5	7.2
Maximum		258.8	75.6	64.8	36.4	9.7	55.5
Mean		118.8	35.5	31.1	17.8	6.6	31.5

K_{Lab} *K* from laboratory permeameter test, K_{KC} *K* from Kozeny-Carmen method, K_{FH} *K* from Fair-Hatch method, *k-darcy* intrinsic permeability (a function/property of aquifer medium only)

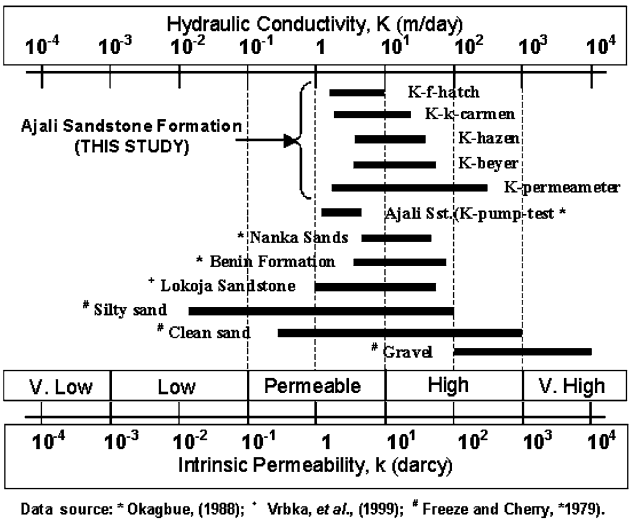

Fig. 7 Permeability evaluation chart showing the range of hydraulic conductivity (*K*) and intrinsic permeability (*k*) from the different estimation approach

of interpretation of the overall data trend (Massart and Kaufman 1983; Simeonov et al. 2003). Principal component analysis (PCA) is a valuable pattern recognition technique that attempts to explain the variance of a large data set of inter-correlated variables with a smaller set of independent variables, i.e., principal components. Hence *R*-mode principal component analysis (PCA) was employed in this study to characterize the relationship between textural-statistical indices and the different hydraulic conductivity estimates in order to identify possible controlling factors.

As presented in Table 3, the PCA extracted four main principal component factors with eigenvalues >1 summing up to 85% of the total variance in the dataset. Furthermore, only variables with factor score greater than 0.4 are considered significant and as such included in the controlling variables. The first factor, which accounts for 25.4% of the total variance, was loaded in favour of all the empirical-based *K* estimations and graphic mean (G_m). This factor, tagged "empirical *K*-index" revealed the common fundamental basis of the different empirical methods in relation to the average grain size characteristic (G_m) of the unconsolidated sands, in this case, Ajali Formation. The second factor, which weighed positively in favour of the textural parameters such as C_u, C_c, % sand and negatively against % fine could be termed as "textural control" and signifies the textural influence in terms of grain sizes, grading, sorting and packing on the hydraulic conductivity. Nonetheless, the observed negative loading of −0.95 with respect to % fine is a clear indication of inverse relationship and negative influence on the hydraulic conductivity as well as other components of factor-2. The third factor, termed "size-porosity control", was loaded in respect of porosity, skewness as well as D_{10} and D_{50} grain sizes. This clearly underlies the significant association between the grain-size distribution and the porosity of the materials, which in turn will influence the hydraulic conductivity of the granular Ajali Formation materials. The fourth factor was loaded with respect to the permeameter-based *K* values, standard deviation (sorting) and kurtosis. This clearly shows the significant control of kurtosis and sorting on the results of the permeability tests, which can be attributed to the influence of possible resorting during repacking of the

Table 3 Results of factor analysis showing the PC grouping and scores for hydraulic and statistical textural data of the Ajali Formation

Variables	Extracted factor components			
	1	2	3	4
K-Kozeny-Carmen	0.867			0.432
K-Fair-Hatch	0.844			
K-Hazen	0.822	−0.445		
G-Mean	0.806			0.522
K-Beyer	0.794	−0.455		
% Sand		0.953		
% Fine		−0.953		
Uniformity coeff. C_u		0.883		
Coeff. of curvature C_c	−0.529	0.708		
D_{10}: Grain size			0.898	
D_{50}: Grain size			0.761	
Porosity			0.747	−0.464
St. deviation				0.910
Skewness			0.520	−0.606
Kurtosis				0.805
K-Permeameter				0.658
Eigenvalue	5.88	3.20	2.33	1.54
% Cum. variance	25.4	49.3	68.8	85.1

granular unconsolidated Ajali Formation samples in the permeameter tube.

The overall evaluation as presented in Table 3, shows varied inter-dependence of various *K*-estimations with the textural-statistical characteristics of the Ajali Formation. In addition, the textural and hydraulic data set revealed significant positive correlations among the empirical *K*-estimations ($r = 0.53$–0.99). Also the relatively significant positive dependence of the empirically determined *K* values on graphic mean grain size (0.36–0.90), percentage sand content (0.30–0.61) and porosity (0.26–0.56) is a confirmation of the textural controls on the hydraulic characteristics of the granular Ajali Formation. However, the low correlations ($r = 0.01$–0.20) of the empirical *K*-estimations with the laboratory permeameter-based *K* values can be attributed to the marked differences in the textural controls on the respective *K*-values.

Geochemical profiles and weathering characteristics

The summary of the results of the geochemical analyses of the major and trace element concentrations of both fresh and ferruginized samples of Ajali Formation are presented in Table 4, alongside with ratios between some selected elements and estimated weathering indices. Initial mineralogical examination under binocular microscope of selected samples of Ajali Formation revealed the dominance of sub-angular to rounded polycrystalline quartz, while the presence of dispersed whitish fines suggests possible clay cementing material. As expected, the results of the major element geochemistry, as summarized in Table 4, show that the analyzed fresh samples are dominated by quartz with corresponding high proportion of SiO_2 (94.8–99.0 wt.%), while other major oxides are generally below 1.0 wt.%. The results generally revealed similar elemental composition for all samples reflecting the homogeneity of the Ajali Formation as well as a uniform depositional or sedimentary environment.

However, the ferruginized samples, though with similar chemical trend, exhibit elevated concentrations of Al_2O_3 (3.50–11.60 wt.%) and Fe_2O_3 (1.80–3.60 wt.%), which are clear indications of weathering/ferruginization processes. This is clearly supported by the low Si/Al ratio of 6.6–25.8 in the weathered samples compared to the relatively higher values of 37.3–300 for the fresh samples. Furthermore, the plot of the mineralogical and chemical composition of the samples using Silica–Sesquioxides-Alkalis ternary plot as presented in Fig. 8a, shows that all samples lie towards the silica (*Q*) corner, indicating severe depletion of the Sesquioxide and the Alkali. The Al_2O_3–$CaO + Na_2O$–K_2O ternary plot (Fig. 8b), shows the distribution of the studied samples, alongside the primary mineralogy of the source Basement Complex rocks. As indicated, the Ajali Formation samples plot at the Al_2O_3 corner, implying intense primary weathering process and removal of feldspars and other mobile elements that characterized the primary source rock materials. However, cross plots of Fe + Mg and K/Na ratio (Fig. 9a), as well as chemical weathering index (CIA) against $\%SiO_2$ (Fig. 9b), demonstrate the secondary weathering process and enrichment of Fe and Mg in the ferruginized samples compared to the fresh samples. Therefore, it can be concluded that the depletion of all other major and some trace elements in the Ajali Formation are related to the removal of ferromagnesian minerals and feldspars through reworking and transportation of the source materials during sedimentary process.

Investigations of siliciclastic sedimentary rocks in several regions of the world show that their chemical composition is largely dependent on the composition of the weathering conditions at the source area (Nesbitt and Young 1982, 1989; Nesbitt et al. 1996). Hence, based on the profiles of the geochemical data presented above, assessment of the degree of weathering and provenance setting were undertaken. As demonstrated by Nesbitt and Young (1982), a measure of the degree of chemical weathering/alteration of the sediments' source rocks can be constrained by calculating the chemical index of alteration (CIA), [where CIA = molar $Al_2O_3/(Al_2O_3 + CaO^* + Na_2O + K_2O)$] while CaO* represents the amount of CaO in silicate minerals only [i.e., excluding those of carbonates

Table 4 Summary of geochemical analyses results of the major oxides including some selected elemental ratios and weathering indices for the Ajali Formation samples

Parameters	Fresh samples ($N = 12$)					Ferruginized samples ($N = 4$)				
	Min.	Max.	Mean	Median	St. Dev.	Min.	Max.	Mean	Median	St. Dev.
SiO_2%	94.8	98.9	97.2	97.3	1.20	76.	91.9	83.8	80.2	7.24
Al_2O_3%	0.33	2.56	1.16	0.97	0.61	3.56	11.6	7.93	10.2	3.92
Fe_2O_3%	0.03	0.59	0.23	0.19	0.17	1.80	3.57	2.70	2.96	0.79
TiO_2%	0.04	0.84	0.24	0.16	0.24	0.32	1.03	0.74	0.90	0.34
MnO%	bdl	0.01	0.01	0.01	0.00	0.01	0.01	0.01	0.01	0.00
MgO%	0.01	0.05	0.02	0.01	0.01	0.02	0.04	0.03	0.03	0.01
CaO%	0.01	0.06	0.02	0.01	0.02	0.01	0.02	0.01	0.01	0.00
Na_2O%	0.01	0.04	0.02	0.01	0.01	0.01	0.02	0.01	0.01	0.001
K_2O%	bdl	0.08	0.03	0.04	0.02	0.01	0.03	0.03	0.03	0.01
P_2O_5%	bdl	0.02	0.01	0.01	0.00	0.01	0.06	0.04	0.06	0.02
ZrO2%	bdl	0.13	0.04	0.03	0.03	0.02	0.11	0.07	0.06	0.04
LOI	0.06	2.34	1.07	1.06	0.63	2.36	6.88	4.69	5.61	2.17
Rb (ppm)	0.67	123.2	34.5	1.56	47.2	3.37	4.08	3.67	3.56	0.37
Sr (ppm)	7.14	13.3	9.69	8.96	2.08	17.2	75.0	54.5	71.	32.4
Ba (ppm)	7.32	25.1	19.8	23.1	6.43	25.9	58.1	46.9	57.1	18.3
Si/Al	37.3	299.9	113.5	100.6	74.2	6.64	25.8	14.4	7.88	9.68
Na/K	0.17	5.00	1.42	0.88	1.64	0.33	1.00	0.53	0.33	0.30
Fe/Mg	3.0	59.0	18.1	11.8	15.	81.3	98.7	91.2	90.0	6.96
Zr/Ti	0.06	0.73	0.22	0.17	0.17	0.08	0.18	0.12	0.13	0.04
% CIA	86.8	98.6	93.7	93.4	3.60	98.3	99.6	99.2	99.4	0.51
% CIW	93.5	99.1	96.5	96.9	1.84	99.2	99.8	99.6	99.7	0.28

Bdl below detection limit, *LOI* loss of ignition, *CIA* chemical index of alteration after Nesbitt and Young 1982, *CIW* chemical index of weathering after Harnois 1988

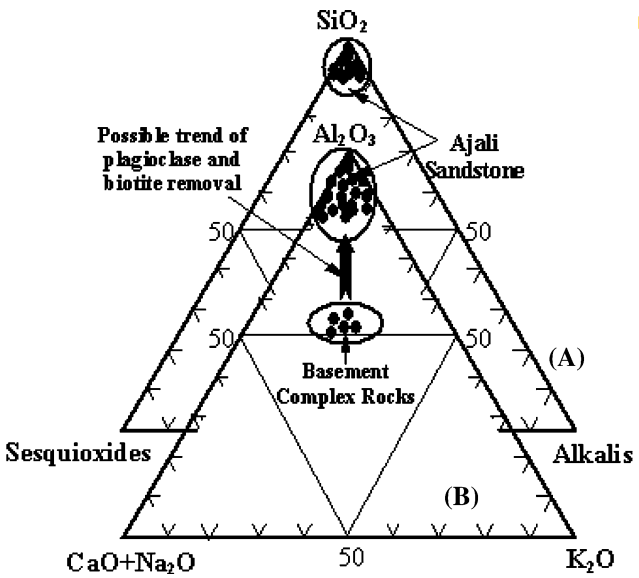

Fig. 8 Average mineralogical and chemical composition of the Basement Complex rocks alongside with ASF samples plotted on: (*A*) Silica–Sesquioxides-Alkalis and (*B*) Al_2O_3–CaO + Na_2O–K_2O ternary diagrams (Note: *bold arrow* indicates trend of plagioclase and biotite removal during weathering and transportation processes)

which are incidentally not presented in the fluvio-continental Ajali Formation as indicated by very low content of CaO (0.1–0.04%)]. Also the proposed chemical index of weathering (CIW) of Harnois 1988, is similar to the CIA with the exception of exclusion of K_2O in the equation [CIW = molar $Al_2O_3/(Al_2O_3 + CaO^* + Na_2O + K_2O)$]. Usually, the CIA or CIW are interpreted in similar way with values of about 50, for unweathered (fresh) upper crust material and about 100, for highly weathered residual soils.

In this study, the estimated CIA and CIW (see Table 4) yielded values in the range of 86.8–99.6 for the fresh samples and 98.3–99.6 for the ferruginized samples. The values >98 for the ferruginized samples are obviously expected, while Fe/Mg values of 81.3–98.7, compared to 3.0–59.0 for fresh samples clearly confirm the weathering-ferruginization process. However, relatively high values of CIA and CIW (86.8–99.6) for the fresh samples is an indication of the fact that the primary source material(s) must have been subjected to substantially high degree of weathering and reworking that had resulted in the removal of the ferromagnesian minerals and feldspars. Therefore, it can be deduced that the CIA and CIW values for the ferruginized samples reflect the recent (secondary) weathering-ferruginization process, while that of the fresh samples are reflections of primary weathering of the source materials.

To assess the possible impact of the above secondary weathering-ferruginization process in terms of metal

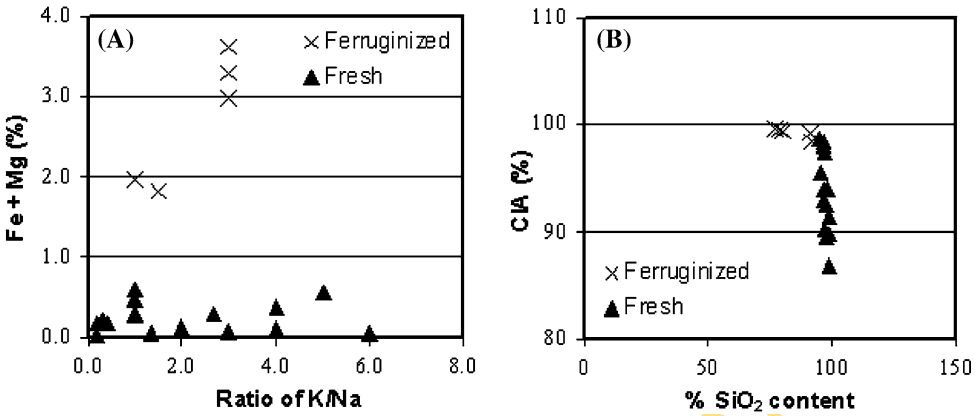

Fig. 9 Correlation plot of (**a**) (Fe + Mg) against K/Na ratio and (**b**) chemical index of alteration (CIA) against silica contents

enrichment, a summary of the metal concentrations in both fresh and ferruginized units are presented in Table 5. As shown in Table 5, there are only slight differences in the concentrations of the major elements between the fresh and ferruginized units of Ajali Formation. However, the trace metals (Ba, Sr, Cu, Pb, Zn, Cr, Co, and Ni) exhibited about 2–5 folds increase in the ferruginized units compared to the concentrations in the fresh Ajali Formation. Such trace metals profile of the weathered samples are consistent with trace metals association (Cr, Co, Cu, As, Pb, Zn, Mn, and Mo) in ferruginous regolith as outlined by Roquin et al. (1990) and Butt and Smith (1992). The potential for enrichment of such trace/heavy metals could be related to the formation of Fe oxides/oxyhydroxide as shown by the following relation:

a) Under oxidizing condition (i.e., unsaturated/phreatic zone of the aquifer)

$$Fe^{2+} + {}^{1}/_{2}O_2 + H_2O = Fe(OH)_2$$
$$4Fe^{2+} + O_2 + 10H_2O = 4Fe(OH)_3 + H^+$$

b) Under reducing condition (i.e., saturated zone of the aquifer)

$$3Fe^{2+} + 4H_2O = Fe_3O_4 + 4H_2$$

Taylor and Eggleton (2001) noted that the formation of Fe-oxides and oxyhydroxide as shown above dominates weathering process while the ferric hydroxide precipitate is said to be highly reactive due to the large surface area. Consequently, it is this characteristic that makes Fe-oxides and oxyhydroxide alongside with Mn-oxides and Al-hydroxyl complex to serve as sinks capable of adsorbing wide range of trace/heavy metals as observed for the ferruginized samples of Ajali Formation. Further confirmation of this is clearly reflected in the estimated

Table 5 Summary of concentration profiles of major and selected trace metals (mg/kg) alongside estimated enrichment factor (EF)

Parameters	Fresh formation ($N = 12$)			Ferruginized formation ($N = 4$)			Enrichment factor (EF)		
	Min.	Max.	Mean	Min.	Max.	Mean	Min.	Max.	Mean
Ca	71.5	429	143	71.5	143	71.5	0.17	0.27	0.21
Mg	60.3	301.5	120.6	120.6	241.2	180.9	0.33	1.09	0.60
Na	74.2	296.8	148.4	74.2	148.4	74.2	0.17	0.27	0.21
K	bdl	664	249	83	249	249	0.57	4.08	1.83
Si	443758	463086	454943	359377	429905	392184	0.16	0.22	0.18
Fe	209.7	4124.1	1607.7	12582	24954	18873	0.06	10.78	5.34
Mn	bdl	77.5	77.5	77.5	77.5	77.5	0.06	1.67	1.02
Ba	7.32	25.1	19.8	25.9	58.1	47.0	0.26	0.87	0.50
Sr	7.14	13.3	9.7	17.2	75.0	54.5	0.40	1.81	0.91
Cu	0.01	1.16	0.27	3.07	3.73	3.5	0.59	98.95	50.24
Pb	2.05	4.43	3.05	8.01	15.6	12.3	0.62	1.08	0.92
Zn	2.66	6.78	4.37	7.2	15.2	11.6	0.45	0.50	0.48
Co	0.01	0.66	0.22	0.78	2.79	1.87	6.43	53.55	24.33
Cr	5.09	12.8	9.42	17.9	58.5	42.9	0.59	1.41	1.06
Ni	1.52	3.66	2.53	5.41	12.4	9.3	0.42	1.19	0.83

Bdl below detection limit

enrichment factors (EF) normalized with respect to immobile Ti based on the following relation:

$$EF = [(Me/Ti)_{weatheredunit}/(Me/Ti)_{freshunit}]$$

whereby; Me is the respective trace metal of interest and Ti is the reference immobile element in weathered unit on one hand and fresh bedrock on the other hand. EF value of approximately 1 for any element/metal imply concentration representing the geogenic input, while EF >1 and EF <1 indicate enrichment and depletion respectively of the affected metal.

Using the above relation, the estimated normalized enrichment factor (EF) presented in Table 5, revealed that only K, Fe, Mn, Co and Cr exhibited enrichment in the ferruginised units (EF of 1.01–50.24). Such enrichment can be attributed to the highly reactive (large surface area) oxides/oxyhydroxides of Fe and Mn responsible for the common reddish-brownish coloration of the ferruginized units. In addition, studies had shown that such oxides/oxyhydroxides of Fe and Mn and associated clay minerals do serve as sinks/hosts for a wide range of trace/heavy metals such as Cu, Co, and Cr as observed for the ferruginized Ajali Formation (Sharma and Rajamani 2000; Taylor and Eggleton 2001). Hence, the observed ferruginization enrichment of trace metals, in this study, is an indication of possible/potential threats to groundwater quality. This arises from the fact that infiltration/recharge induced geochemical redox process can further enhance the dissolution and redistribution of such trace/heavy metals into the groundwater (Bruand 2002).

Metals mobility and groundwater quality

From the overall assessment as presented so far, there is no doubt as to the high aquiferous potentials of the ASF in terms of storage capacity and yield. This is adequately supported by the estimated average porosity of about 27% as well as by the estimated and laboratory hydraulic conductivity (K) values in the range of 1.2×10^{-5}–1.2×10^{-3} m/s. Such prolific hydraulic characteristics alone are not enough in terms of comprehensive management of groundwater and aquifer system, which should also take the quality aspect of the groundwater into consideration. Consequently, it should be pointed out that weathering-ferruginization processes constitute a significant source of trace metals release into the environment and possible enrichment of the mobilized metals in soils (aquifer), surface and groundwater systems. The dynamics of such ferruginization-weathering products are said to be partly controlled by percolating/recharging water and surface erosion (Taylor and Eggleton 2001). Therefore, in this section, brief highlight of the possible influence of weathering-induced geochemical interactions between the groundwater and the aquifer materials of the ASF is presented.

A general look at the chemical profiles of the groundwater samples from 10 different locations within the Ajali Formation as presented in Table 6, indicates that both major and trace metal concentrations are within the limits of WHO (1993) and Standard Organization of Nigeria, SON (2007) standards for drinking water quality. The respective low concentrations of the metals, alongside with the low EC values of 14–268 μs/cm, imply low mineralized water from clean sandy aquifer devoid of labile and weatherable minerals. However, a closer look at the chemical data revealed a clear distinction between the deep boreholes (110–120 m) tapping the fresh aquifer unit and the shallow boreholes (20–30 m) tapping the ferruginized unit. The pH of the water samples from the fresh aquifer unit range between 6.9 and 8.7 and characterized by low EC values of 14–34 μs/cm, However, water samples from the ferruginized unit exhibit slightly higher acidity and dissolved solid with pH values of 5.2–6.5 and EC values of 115–268 μs/cm, Also the water samples from the ferruginized unit exhibit relatively higher concentrations of the major elements (Ca, Mg. Na. K including Ba and Sr) compared to those from the fresh aquifer unit (see Table 6).

The observed distinctions may be attributed to the possible impact of the rapid and intense ferruginization of the Ajali Formation, as observed in the exposed sections in the field, Hence, the observed average composition of 7.93 and 2.7 wt.% for Al_2O_3 and Fe_2O_3, respectively in the ferruginized units compared to values of 1.2 and 0.2 wt.%, respectively in the fresh units can be attributable to infiltrating/recharge water-mediated weathering processes. Consequently, environmental implication in terms of possible ferruginization-induced release of metals through such weathering-induced geochemical processes is further highlighted by estimation of potential metal mobilization factor using the following relation modified after Minarik et al. (1998):

$$MF = \frac{cMe_{(water)}}{cMe_{(rock)}} \times \frac{cAl_{(rock)}}{cAl_{(water)}}$$

whereby;

$cMe_{(water)}$ average conc. of respective metal in the groundwater system (mg/l);

$cMe_{(rock)}$ average conc. of respective metal in the aquifer horizon in mg/kg;

$cAl_{(water)}$ average conc. of Al in the groundwater system (mg/l);

$cAl_{(rock)}$ average conc. of Al in the aquifer horizon in mg/kg.

Using the above relation, the average concentrations of the respective metals in the analyzed groundwater samples

Table 6 Concentration profiles of major (mg/l) and trace metals (μg/l) in the analyzed groundwater samples from the Ajali Formation aquifer

Parameters	Fresh aquifer unit							Ferruginized unit			WHO/SON
	L1	L3	L4	L5	L6	L9	L10	L2	L7	L8	
Temp. °C	23.6	27.4	28.4	27.4	27	28.1	27.8	29.4	28	29.2	Variable
pH	8.7	7.4	7.5	6.7	7.2	6.9	6.9	5.24	6.5	6.5	6.5–9.5
EC (μS/cm)	14	19	17.5	21	31	23	34	268	133	115	400–1480
Ca (mg/l)	0.9	0.8	1.2	0.7	1.0	0.3	0.4	7.0	10.7	10.6	75–200
Mg (mg/l)	0.3	0.3	0.3	0.2	0.7	0.3	0.4	6.4	2.8	2.8	50–150
Na (mg/l)	1.4	2.3	1.2	1.6	2.2	0.7	1.1	22.3	14.5	14.4	20–200
K (mg/l)	0.2	0.3	0.4	0.4	1.9	0.3	0.3	13.5	3.1	3.1	10–12
Si (mg/l)	5.2	5.4	6.2	5.5	5.3	5.6	5.7	32.6	5.6	5.7	
Fe (mg/l)	0.35	0.04	1.12	0.03	1.24	0.02	0.03	0.14	0.19	0.2	0.3–1.0
Mn (mg/l)	0.04	0.01	0.03	0.02	0.06	0.03	0.03	0.27	0.12	0.11	0.2
Ba (μg/l)	20	20	20	20	20	20	20	250	50	50	700
Sr (μg/l)	10	10	10	10	10	10	10	100	40	40	
Cu (μg/l)	2	2	21	94	85	17	83	3	2	2	200
Pb (μg/l)	10	10	10	10	60	10	10	10	10	10	10
Zn (μg/l)	43	137	47	25	463	22	140	92	14	17	300
Co (μg/l)	2	2	2	2	2	2	3	14	2	2	
Cr (μg/l)	20	20	20	20	20	20	20	20	20	20	50
Ni (μg/l)	5	5	5	5	5	5	5	14	5	5	20

WHO (1993)—Guidelines for Drinking Water Quality, SON (2007)—Standard Organization of Nigeria: Standards for Drinking Water Quality
L1 Abocho, *L2* Dekina, *L3* Anyangba, *L4* Iyale, *L5* Nsukka, *L6* Igbo-Etiti, *L7* 9th-Mile I, *L8* 9th Mile II, *L9* Okigwe I, *L10* Okigwe II (see location in Fig. 4)

from the fresh and ferruginized units were used for the estimation of respective metal mobilization factor (MF) in respect of the rock/aquifer unit (Table 7). A general look at the estimated MF indicates that the potentials for mobilization of the major cations (Ca, Mg, Na, K) and the selected trace metals (Mn, Fe, Ba, Sr, Cu, Pb, Zn Co, Cr and Ni) from the rock/aquifer are higher. However, the ferruginized unit exhibited higher MF in respect of the major elements, while the fresh unit exhibited MF with respect to the trace elements including Fe. The higher MF with respect to the ferruginized units for most of the major elements including Mn, Ba and Sr is a clear indication of weathering-induced release, while the higher MF for the trace elements including Fe with respect to the fresh aquifer unit may be attributed to higher mobility potentials of metals under reducing conditions in deep aquifer compared to possible fixation in metal-oxides/hydroxide under possible oxic condition in shallow aquifer unit.

In addition, the generally lower mobilization of Si, Fe and Mn under both fresh and ferruginized units (<50), compared to other major elements (56–8,356), may be partly due to the low solubility of Si and possible immobilization of Fe and Mn in form of oxides and oxyhydroxides within the aquifer matrix. Again, a comparison of the metal mobility, in form of mobilization ratio (MR), revealed that the degree of mobility for the major elements including Ba and Sr (with exception of Fe) is about 2–36 folds higher under ferruginized setting (see Table 7). The relatively higher degree of mobilization for Fe and trace elements in the fresh aquifer unit compared to the ferruginized unit is an indication of possible geochemical water-rock interactions (especially reduction of Fe- and Mn-oxyhydroxides), leading to higher metal mobility under reducing condition found in deep aquifer. This is consistent with the study of Quantin et al. (2002), which revealed that under reducing condition, typical of groundwater environment, chemical and bacterial processes do lead to reduction of Mn-oxide and hence the release of Co and Ni associated with the Mn-oxide lattice. Therefore, it can be inferred that the relatively higher MF of the trace metals (Pb, Zn, Cu, Co, Cr and Ni) with respect to the fresh Ajali units may be related to similar reduction of Fe-/Mn-oxyhydroxides, which serve as sinks/hosts for such trace metals.

Consequently, possible remobilization through infiltration-induced leaching processes is a clear indication of the potential environmental impact in terms of groundwater quality as well as borehole/aquifer management, especially under humid tropical environment of the study area. Apart from the fact that formation of Al-, Fe- and Mn-oxides are associated with contaminant trace metals as mentioned earlier, their formation can lead to reduction in the

Table 7 Results of the estimated metal mobilization factors with respect to fresh and ferruginized Ajali Formation aquifer

Parameters	Fresh formation			Ferruginized formation			*M*-ratio
	Av. GW (mg/l) $N = 7$	Av. AU (mg/kg) $N = 12$	MF	Av. GW (mg/l) $N = 3$	Av. AU (mg/kg) $N = 4$	MF	
Ca	0.8	143	136.9	9.4	71.5	4896	35.8
Mg	0.4	120.6	76.6	4.0	180.9	820.6	10.7
Na	1.5	148.4	261.3	17.1	74.2	8536	32.7
K	0.5	249	56.4	6.6	249	978.7	17.4
Si	5.6	454943	0.3	14.6	392184	1.4	4.4
Fe	0.40	1607.7	6.5	0.18	18873	0.3	0.1
Mn	0.03	77.5	10.5	0.17	77.5	49.8	4.7
Ba	0.02	19.78	26.1	0.12	46.97	92.4	3.5
Sr	0.01	9.69	26.7	0.06	54.51	40.9	1.5
Cu	0.04	0.27	4117	0.00	3.48	24.5	0.0
Pb	0.02	3.05	144.1	0.01	12.31	30.2	0.2
Zn	0.13	4.37	739.9	0.04	11.62	130.9	0.2
Co	0.00	0.22	232.0	0.01	1.85	120.6	0.5
Cr	0.02	9.42	54.9	0.06	42.92	51.9	0.9
Ni	0.01	2.53	51.1	0.01	9.33	31.8	0.6

MF mobilization factor, *M-ratio* mobilization ratio w.r.t. ferruginized unit, *Av. GW* average composition of the respective groundwater system, *Av. AU* average composition of the respective rock (aquifer) unit

permeability of the filter/gravel layers around the intake portion of the boreholes and thus reduce the efficiency or yield on one hand. On the other hand, reduction-oxidation processes involving such Fe-Mn-Al-oxyhydroxides can lead to chemical reactions characterized by precipitation, encrustation and corrosion of the well (borehole) materials. Detail assessment of such flow-induced geochemical processes related to iron-oxidation, corrosion and encrustation in water wells are presented elsewhere in Tijani 1996.

Finally, it should be pointed out that the foregoing discussion in respect of the geochemical interactions and attendant groundwater quality problems is by no means exhaustive; hence a detailed geochemical modeling of the overall groundwater-aquifer interactions involving leaching tests at different pH and redox conditions can be seen as the focus of future study.

Summary and conclusion

In this study, assessments of the textural, hydraulic and geochemical characteristics of Ajali Formation were undertaken. The results indicate the Ajali Formation to be well sorted fine to medium grained sands, with minor amounts of silt. The evaluated textural parameters (Cu = 1.5–3.4, n = 18–32% and D_{10} = 0.1–0.25 mm) in addition to statistical parameters (such as skewness, kurtosis, graphic mean etc.) are indications of high aquiferous potentials of the Ajali Formation in terms of the groundwater occurrence. For the comparative assessment of the estimated *K*-values, the overall evaluation shows varied inter-dependence of various *K*-estimations with the textural-statistical characteristics of the Ajali Formation. In addition, the multivariate factor analysis of the textural and hydraulic data set revealed the significant positive correlations among the empirical *K*-estimations (r = 0.53–0.99). The relatively significant positive dependence of the empirically determined *K* values on graphic mean grain size (0.36–0.90), percentage sand content (0.30–0.61) and porosity (0.26–0.56) are consistent with the PCA component factors as outlined in Table 3 and also underly the reliability of the empirical estimation employed in this study.

Furthermore, the assessment of the degree of weathering revealed that the CIA and CIW values for the ferruginized samples reflect the recent (secondary) weathering-ferruginization process, while that of the fresh samples are reflections of the primary weathering of the source materials of the Ajali Formation. However, while the textural characteristics exert positive impacts on groundwater occurrence and recharge, the geochemical components of the ferruginized Ajali Formation in respect of the weathering-induced enrichment of metals signify possible negative impacts on groundwater quality. The groundwater is generally soft, slightly acidic, and low in dissolved solids; silica makes up a large part of the dissolved constituents, hence, the major processes affecting groundwater composition are the dissolution process mediated by CO_2-charged infiltrating rainwater and the associated weathering/ferruginization process. Assessment of the potential metal mobilization revealed higher MF with respect to the ferruginized aquifer unit for most of the major elements including Mn, Ba and Sr, which is a clear

indication of weathering-induced release. However, the observed higher MF for the trace elements including Fe with respect to the fresh aquifer unit may be attributed to the relatively higher mobility potentials of metals under reducing conditions in deep aquifer compared to possible fixation in metal-oxides/hydroxides under possible oxic condition in shallow aquifer unit.

The overall assessment presented in this study, suggests interplay of grain-size, textural and hydraulic characteristics as the dominant controlling factors in terms of groundwater occurrence. However, weathering induced geochemical processes with resultant formation of Fe-Mn-Al-oxyhydroxides and leaching/dissolution mobilization of metals including contaminant trace metals constitute potential aquifer management problems in terms of water quality and well (borehole) deterioration, through encrustation and clogging of the effective interstitial pore spaces. Thus, this underlies the need to adequately understand the interrelationship between the textural, hydraulic, geochemical and weathering characteristics of aquifer materials in respect to overall groundwater or aquifer management.

Acknowledgments The authors acknowledge with thanks the donation of the laboratory permeameter set-up used in this study by Prof. K. Jinno (Institute of Environmental Systems, Kyushu University, Fukuoka, Japan) while the assistance of Mr. K. Watanabe and Prof. Kitagawa (Department of Earth and Planetary Science Systems, Hiroshima University, Japan) in respect of the XRF analyses is also appreciated. The assistance of Toyin Alli and Ben Obinwa in the field sampling and laboratory permeameter tests is gratefully commendable, while the useful suggestions of Prof. E.P. Loehnert (Muenster, FRG) and the comments of the anonymous reviewers are also thankfully appreciated. Finally, the benefit of JSPS fellowship support to the first author, during which this manuscript was prepared is gratefully acknowledged.

References

Adediran SA, Adegoke OS, Oshin IO (1991) The continental sediments of the Nigerian Coastal Basins. J Afr Earth Sci 12(1–2):79–84

Agagu OK, Fayose EA, Petters SW (1985) Stratigraphy and sedimentation in the Cenomanian Anambra Basin, Eastern Nigeria. Niger J Min Geol 23:25–36

Alyamani MS, Sen Z (1993) Determination of hydraulic conductivity from complete grain-size distribution curves. Ground Water 31(4)

Amajor LC (1987) Paleocurrent, petrography and provenance analyses of the Ajali Sandstone (Upper Cretaceous), southeastern Benue Trough, Nigeria. Sediment Geol 54:47–60

Angeroth CE (2002) Characterization of hydraulic conductivity of the alluvium and basin fill, Pinal Creek Basin near Globe, Arizona. USGS Water-Resources Investigations Report 02–4205, 15 pp, Tucson

Appelo C, Postma D (2005) Geochemistry, groundwater and pollution. Balkema, Amsterdam

Benkhelil J (1986) Structure and geodynamics evolution of the intracontinental Benue-Trough (Nigeria). PhD Thesis, Univ. Nice, 202 p, Pub. Elf (Nig.) Ltd

Beyer W (1964) Zur Bestimmung der Wasserdurchlaessigkeit von Kiesen und Sanden aus der Kornverteilungskurve. Wasserwirtschaft, Wassertechnik 14:165–168

Bouwer H, Rice RC (1976) A slug test for determining hydraulic conductivity of unconfined aquifers with completely or partially penetrating wells. Water Resour Res 12(3):423–428

Bruand A (2002) Concentration and mobility of lithogenic trace metals in soils: Significance of anthropogenic lateral redistributions. CR Geosci 334:581–582

Budhu M (2000) Soil mechanics and foundations, Wiley, London

Burke KC, Dessauvagie TFJ, Whiteman AJ (1972) Geological history of the Benue valley and adjacent areas. In: Dessauvagie TFJ, Whiteman AJ (eds) African geology. University of Ibadan Press, Nigeria, pp 187–218

Butler JJ Jr (1997) The design, performance, and analysis of slug tests. Lewis Publishers, Boca Raton, 272 p

Butler JJ Jr., Garnett EJ (2000) Simple procedures for analysis of slug tests in formations of high hydraulic conductivity using spreadsheet and scientific graphics software: Kansas Geological Survey Open-File Report 2000–40, 20 p

Butt CRM, Smith RE (1992) Characteristics of the weathering profile. In: Butt CRM, Zeegers H (eds) Regolith exploration geochemistry in Tropical and Sub-tropical Terrains. Elsevier, Amsterdam, pp 299–304

Carmen PC (1939) Permeability of saturated sands, soils and clays. J Agric Sci 29:263–273

Cratchley CR, Jones JP (1965) An interpretation of the geology and gravity anomalies of the Benue Valley, Nigeria. Overseas Geol Surv Geophys Pap 1:1–26

Darcy H (1856) Les Fontaines Publiques de la Ville de Dijon, Dalmont, Paris

Egboka BCE, Uma KO (1986) Comparative analysis of transmissivity and hydraulic conductivity values from the Ajali aquifer system of Nigeria. J Hydrol 82(1–2):185–196

Fair GM, Hatch LP (1933) Fundamental factors governing the streamline flow of water through sand. J Am Water Works Assoc 25:1551–1565

Freeze RA, Cherry JA (1979) Groundwater. Prentice Hall, Englewood Cliffs, NJ, 604 p

Folks RL, Ward WC (1957) Brazo river bar: a study of the significance of grain size parameters. J Sediment Geol 27:3–26

Glynn PD, Plummer LN (2005) Geochemistry and the understanding of ground-water systems. Hydrogeol J 13:263–287

Harnois L (1988) The CIW index: a new chemical index of weathering. Sediment Geol 55:319–322

Hazen A (1892) Some physical properties of sands and gravels. Mass. State Board of Health, 24th Annual Report, pp 539–556

Hazen A (1930) Water supply, American civil engineers handbook. Wiley, New York, pp 1444–1518

Hoque M, Ezepue MC (1977) Petrology and palaeogeography of the Ajali Sandstone. J Min Geol 14(1):6–22

Hudson RO, Golding DL (1997) Controls on groundwater chemistry in subalpine catchments in the southem interior of British Columbia. J Hydrol 20l:1–20

King LC (1950) Outline and disruption of Gondwanaland. Geol Mag 87:353–359

Krumbein WC, Monk GD (1942) Permeability as a function of the size parameters of unconsolidated sand. Am Inst Mining Eng, Littleton, CO, Tech Pub, pp 153–163

Ladipo KO (1986) Tidal shelf depositional model for the Ajali Sandstone, Anambra Basin, Southern Nigeria. J Afr Earth Sci 5(2):177–185

Ladipo KO (1988) Paleogeography, sedimentation and tectonics of the upper cretaceous Anambra basin, southeastern Nigeria. J Afr Earth Sci 7(5–6):865–871

Lee SS (1998) Estimation of hydraulic conductivity from grain size, grain shape, and porosity. http://www.vadose.net/hycunduc.html#top

Llyod JW, Heathcote JA (1985) Natural inorganic hydrochemistry in relation to groundwater: an introduction. Clarendon Press, Oxford; 296 p

Massart DL, Kaufman L (1983) The interpretation of analytical chemical data by the use of cluster analysis. Wiley, NY

MacDonald A, Davies J, Calow R, Chilton J (2005) Developing groundwater: a guide for rural water supply. ITDG Publishing, UK, 358 p

Minarik L, Zigova A, Bendl J, Skrivan P, Stastny M (1998) The behaviour of rare-earth elements and Y during the rock weathering and soil formation in the Ricany granite massif, central Bohemia. Sci Total Environ 215:101–111

Murat RC (1972) Stratigraphy and palaeogeography of the Cretaceous and Lower Tertiary in southern Nigeria. In: Dessauvagie TFJ, Whiteman AJ (eds) African geology, pp 251–266

Nesbitt HW, Young GM (1982) Early Proterozoic climates and plate motions inferred from major element chemistry of lutites. Nature 299:715–717

Nesbitt HW, Young GM (1989) Formation and diagenesis of weathering profiles. J Geol 97:129–147

Nesbitt HW, Young GM, McLennan SM, Keays RR (1996) Effect of chemical weathering and sorting on the petrogenesis of siliciclastic sediments, with implications for provenance studies. J Geol 104:525–542

Nwachukwu SO (1972) The tectonic evolution of the southern portion of the Benue-trough. Geol Mag 109:411–419

Nwajide CS (1979) A lithostratigraphic analysis of the Nanka Sands, southeastern Nigeria. J Min Geol 16:103–109

Nwajide CS, Hoque M (1979) Gullying processes in southeastern Nigeria. Niger Field XLIV:64–74

Obaje NG, Ulu OK, Petters SW (1999) Biostratigraphic and geochemical controls of hydrocarbon prospects in the Benue Trough and the Anambra Basin, Nigeria. NAPE Bull 14(1):18–54

Okagbue CO (1988) Hydrology and chemical characteristics of surface and groundwater resources of the Okigwe Area and Environs, Imo State, Nigeria. In: Ofoegbu CO (ed) Groundwater and mineral resources of Nigeria. Friedr Vieweg & Sohn, Braunschweig/Weisbaden, pp 3–15

Quantin C, Becquer T, Berthelin J (2002) Mn-oxide: a major source of easily mobilisable Co and Ni under reducing conditions in New Caledonia Ferrasols. CR Geosci 334:273–278

Reyment RA (1965) Aspects of geology of Nigeria, Univ Ibadan, Press, 145 p

Roquin C, Freyssinet Ph, Zeegers H, Tardy Y (1990) Elements distribution patterns in laterites of southern Mali: consequences for geochemical prospecting and mineral exploration. Appl Geochem 5:303–315

Sharma A, Rajamani V (2000) Weathering of gneissic rocks in the upper reaches of Cauvery River, south India: implications to neotectonics of the region. Chem Geol 166:203–223

Shephered RG (1989) Correlations with permeability and grain size. Ground Water 27(5)

Simeonov V, Stratis JA, Samara C, Zachariadis G, Vousta D, Anthemidis A, Sofoniou M, Kouimtzis Th (2003) Assessment of the surface water quality in Northern Greece. Water Res 37:4119–4124

Smedley PL, Kinniburgh DG (2002) A review of source, behaviour and distribution of arsenic in natural waters. Appl Geochem 17:517–568

SON (2007) Nigerian Standards for Drinking Water Quality. Standard Organization of Nigeria (SON) Publ. NIS-554; 30 p

Taylor GR, Eggleton RA (2001) Regolith geology and geomorphology. Wiley, NY, 375 p

Tijani MN (1996) Iron in shallow ground water in Moro Area, Kwara State, Nigeria. Water Int 21(4):206–212

Tijani MN, Okunlola OA, Abimbola AF (2006) Lithogenic concentrations of trace metals in soils and saprolites over crystalline basement rocks: a case study from SW Nigeria. J Afr Earth Sci 46:427–438

Tóth J (1999) Groundwater as a geologic agent: an overview of the causes, processes, and manifestations. Hydrogeol J 7:1–14

Uma KO, Onuoha KM (1988) Groundwater fluxes and gully development in S.E. Nigeria. In: Ofoegbu CO (ed) Groundwater and mineral resources of Nigeria. Friedr. Vieweg & Sohn, Braunschweig/Weisbaden, pp 39–59

Uma KO, Egboka BCE, Onuoha KM (1989) New statistical grain-size method for evaluating the hydraulic conductivity of sandy aquifers. J Hydrol 108:343–366

Vrbka P, Ojo JO, Gebhardt H (1999). Hydraulic characteristics of the Maastrichtian sedimentary rocks of the southeastern Bida Basin, central Nigeria. J Afr Earth Sci 29(4):659–667

WHO (1993) Guidelines for Drinking Water Quality–2. WHO, Geneva